Carbohydrate Polymers 121 (2015) 199–206

Contents lists available at ScienceDirect

Carbohydrate Polymers

journal homepage: www.elsevier.com/locate/carbpol

Hypoglycemic activity and potential mechanism of a polysaccharide from the loach in streptozotocin-induced diabetic mice

Jun Zhou*, Junyan Yan, Zhaoshuai Bai, Kaicheng Li, Kaixun Huang*

Hubei Key Laboratory of Bioinorganic Chemistry and Materia Medica, School of Chemistry and Chemical Engineering, Huazhong University of Science and Technology, 1037 Luoyu Road, Wuhan 430074, PR China

ARTICLE INFO

Article history:
Received 20 August 2014
Received in revised form
12 December 2014
Accepted 15 December 2014
Available online 2 January 2015

Keywords:
Misgurnus anguillicaudatus polysaccharide
Diabetes
Insulin
Dyslipidemia
Oxidative stress
Inflammation

Chemical compounds studied in this article:
Streptozotocin (PubChem CID: 29327)
Glucose (PubChem CID: 5793)
Metformin (PubChem CID: 4091)
Cholesterol (PubChem CID: 5997)
Malondialdehyde (PubChem CID: 10964)
Glutathione (PubChem CID: 124886)

ABSTRACT

The present study was designed to investigate the hypoglycemic activity and the potential mechanisms of *Misgurnus anguillicaudatus* polysaccharide (MAP) in streptozotocin-induced diabetic mice. MAP oral administration significantly decreased the blood levels of glucose, TC, TG, LDL-C, and increased the blood levels of HDL-C and insulin in diabetic mice, concurrent with increases in body weights and pancreatic insulin contents. Moreover, MAP reversed the increased mRNA expressions of PEPCK and the reduced glycogen contents in the liver of diabetic mice. Concurrently, MAP exhibited potent anti-inflammatory and anti-oxidative activities, as evidenced by the decreased blood levels of TNF-α, IL-6, monocyte chemoattractant protein-1, MDA, and also the elevated SOD and GPx activities in the serum of diabetic mice. Furthermore, MAP also significantly improved the blood markers of the impaired liver function and renal function in diabetic mice. Altogether, these results suggest that MAP may be a potential therapeutic option for type 1 diabetes.

1. Introduction

The loach (*Misgurnus anguillicaudatus*) serves as a kind of delicious nutritive food and also has long been employed as Chinese traditional medicine in folk remedies for the treatment of hepatitises, carbuncles, osteomyelitis, inflammation and cancers, as well as for the restoration of health disorders caused by aging and various pathogeneses (Qin, Huang, & Xu, 2002d). Generally, the mucus coat of fish skin contains a variety of secretions from epithelial cells and epidermal goblet cells, which have been implicated in many important biological functions (Whitear, 1984). In line with this, some vertebrate lectins, purified from the skin mucus or egg of the loach, were found to induce release of cytotoxin from macrophages or fresh murine bone narrow cells and lyse tumor cells but not normal spleen cells (Goto-Nance & Watanabe, 1995; Okutumi, Nakajima, Sakakibara, Kawauchi, & Yamazaki, 1987). A novel antimicrobial peptide named misgurin, consisting of 21 amino acid residues, was isolated from the loach and identified (Park, Lee, Park, Kim, & Kim, 1997). Moreover, a deaminated neuraminic acid-containing glycoprotein from the skin mucus of the loach, was isolated and characterized (Kimura et al., 1994).

The biological activities of the polysaccharides and polysaccharide–protein complexes isolated from mushrooms, fungi, algae, yeasts, plants, and animals have attracted more and

Abbreviations: ALT, alanine aminotransferase; ANOVA, analysis of variance; AST, aspartate aminotransferase; BSA, bovine serum albumin; BUN, blood urea nitrogen; BW, body weight; CHD, coronary heart disease; FBG, fasting blood glucose; FT-IR, Fourier transform infrared; GC, gas chromatography; GPx, glutathione peroxidase; HDL-C, high density lipoprotein-cholesterol; IL-6, interleukin-6; LDL-C, low density lipoprotein-cholesterol; MAP, *Misgurnus anguillicaudatus* polysaccharide; MCP-1, monocyte chemoattractant protein-1; MDA, malondialdehyde; M-MLV, molony murine leukemia virus; PBS, phosphate buffered saline; PEPCK, phosphoenolpyruvate carboxyl kinase; RT-PCR, reverse transcription-polymerase chain reaction; SEM, standard error of the mean; SOD, superoxide dismutase; STZ, streptozotocin; TBARS, thiobarbituric acid reactive substances; TC, total cholesterol; TG, triglycerides; TNF-α, tumor necrosis factor-alpha.

* Corresponding authors. Tel.: +86 27 87543532; fax: +86 27 87543632.
E-mail addresses: hustzhj@hust.edu.cn (J. Zhou), hxxzrf@hust.edu.cn (K. Huang).

http://dx.doi.org/10.1016/j.carbpol.2014.12.037
0144-8617/

more attention in the biochemical and medical areas (Hurtley, Service, & Szuromi, 2001). In recent years, our group isolated and identified a free neutral polysaccharide from the mucus of the loach *M. anguillicaudatus* (Qin, Huang, & Xu, 2002c). *M. anguillicaudatus* polysaccharide (MAP) was shown to possess a variety of pharmacological properties including anti-inflammatory, anti-oxidative, anti-cancer and hypoglycemic activities, and enhancement of the immune system in vivo and/or in vitro (Qin, Ding, Huang, & Xu, 2008; Qin, Huang, & Xu, 2002a, 2002b, 2002c, 2002d; Qin, Zhou, Zhao, Huang, & Xu, 2001; Zhang & Huang, 2005a, 2005b, 2006).

Diabetes mellitus is one of the most costly chronic diseases with an estimated worldwide prevalence of 366 million in 2011. In recent years, the anti-diabetic activity of polysaccharides have attracted considerable attention (Chen et al., 2013; Fu et al., 2012; Zhang, Zheng, Zhang, & Hai, 2012; Zhu et al., 2013). Our preliminary study showed that MAP exhibited hypoglycemic effect in streptozotocin (STZ)-induced diabetic mice (Qin et al., 2002a), however, the molecular mechanisms underlying the hypoglycemic effect of MAP remain unclear. Therefore, the present study aimed to investigate the hypoglycemic activity and potential mechanisms of MAP in a STZ-induced diabetic mouse model.

2. Materials and methods

2.1. Materials and reagents

The loach (*Misgurnus anguilliacaudatus*, weight 8 ± 1.5 g, length 8.5 ± 3 cm) was purchased from market in Wuhan City, China. STZ and bovine serum albumin (BSA) were purchased from Sigma Chemical Co. (St. Louis, MO). Mouse TNF-α and IL-6 ELISA kits were purchased from eBioscience (San Diego, CA). Mouse MCP-1 ELISA kit was purchased from ALPCO Diagnostics (Windham, NH). TRIzol reagent was obtained from Invitrogen. Molony murine leukemia virus (M-MLV) reverse transcriptase (200 U) and oligo (dT) were purchased from Promega. 10 mM dNTP was from Roche. 2× SYBR Green PCR Master Mix was obtained from Toyobo (Japan). All other chemicals were of the highest commercial grade available.

2.2. Preparation of MAP

MAP was isolated and purified as described in our previous report (Qin et al., 2002c). It was further identified that the average molecular weight was 130 kDa by gel permeation chromatography; the major structure monomers of MAP were composed of galactose, fucose and mannose (5:4:1) by gas chromatography (GC) (Supplemental Fig. 1A and B); the monomers link each other by α-1,3 bonds through periodate oxidation test, Smith degradation test and Fourier transform infrared (FT-IR) spectrum (Supplemental Fig. 1C). In the periodate oxidation test, no periodate was consumed and no formic acid was produced. In the Smith degradation test, the hydrolyzed product contained monoses only, but no glycerol and erythritol. These data are same as our previous results (Qin et al., 2002c).

Supplemental Fig. 1 related to this article can be found, in the online version, at http://dx.doi.org/10.1016/j.carbpol.2014.12.037.

2.3. Animals

Male Kunming mice (20 ± 2 g) were obtained from Hubei Research Center for Laboratory Animals (Wuhan, China) and allowed one week for environmental acclimation. The mice were housed in a temperature (22 ± 2 °C)-controlled room with a 12-h day/night cycle. Throughout the study period, the mice were allowed free access to food and water ad libitum unless otherwise noted. Animal procedures were approved by the Institutional Animal Care and Use Committee at Huazhong University of Science and Technology, and were performed according to the NIH guidelines (NIH publication #85-23, revised in 1996), as well as the guidelines of the Animal Welfare Act.

2.4. Induction of diabetes in mice

For diabetes induction, mice were fasted overnight and then intraperitoneally injected with 100 mg/kg STZ. STZ was dissolved in freshly prepared sodium citrate buffer (pH 4.5) and immediately injected within 20 min of preparation. Control mice were intraperitoneally injected with citrate buffer alone. Five days after STZ injection the diabetic state was assessed by measuring fasting blood glucose (FBG) concentrations after fasting overnight. Mice with FBG concentrations over 11 mmol/L in addition to polyuria and other diabetic features were considered as diabetic.

2.5. Experimental design

All the mice were randomly divided into six groups with 10 mice in each group. Group 1 served as normal controls and received vehicle only (normal saline). Group 2 served as diabetic control and received vehicle. Group 3 received the standard drug metformin (150 mg/kg body weight). Groups 4, 5 and 6 received MAP at 50, 100 and 200 mg/kg body weight, respectively. The vehicle or test drugs were administered via oral gavage (suspended in normal saline). The treatment with MAP was started 5 days after STZ injection and was lasted for 4 weeks. Body weights and FBG concentrations were monitored weekly. At the end of experimental period the mice were fasted overnight, and then sacrificed by exsanguination under diethyl ether anesthesia. Serum was obtained from the blood by centrifugation, and frozen at -80 °C until analysis. The pancreas and liver from each animal were immediately excised and rinsed in phosphate buffered saline (PBS, pH 7.4), and then stored at -80 °C until analysis.

2.6. Measurement of blood glucose and serum insulin levels

Blood samples for glucose assay were obtained from the tail veins of mice after fasting overnight. Blood glucose was measured with an Accu-check Advantage glucometer and blood glucose test strips (Roche Diagnostics GmbH, Mannheim, Germany). Serum insulin levels were determined by using an insulin ELISA kit with mouse insulin as a standard (ALPCO Diagnostics, Windham, NH) according to the manufacturer's instructions.

2.7. Blood lipid profile, liver function and renal function tests

Aspartate aminotransferase (AST), alanine aminotransferase (ALT), blood urea nitrogen (BUN), creatinine, and blood lipid profiles including triglycerides (TG), total cholesterol (TC), low density lipoprotein-cholesterol (LDL-C), and high density lipoprotein-cholesterol (HDL-C) were determined using commercially available kits from Nanjing Jiancheng Bioengineering Institute (Nanjing, Jiangsu, China) according to the manufacturer's instructions.

2.8. Measurement of pancreatic insulin contents

Pancreatic insulin was extracted by an acid/ethanol method as previously described (Noh et al., 2013). The pancreatic insulin contents were determined using an ELISA kit (ALPCO Diagnostics, Windham, NH) and normalized by protein content.

Table 1
Effect of MAP administration for 4 weeks on FBG levels, body weights and food intake in STZ-induced diabetic mice.

Group	FBG levels (mmol/L)		Body weight (g)		Food intake (g/mouse/day)	
	Initial	Final	Initial	Final	Initial	Final
NC	4.9 ± 0.6	5.2 ± 0.7	25.9 ± 1.9	37.3 ± 2.8	4.6 ± 0.5	4.9 ± 0.6
DC	21.9 ± 2.7[b]	23.1 ± 2.8[b]	24.9 ± 1.8	25.8 ± 2.0[b]	4.8 ± 0.6	8.8 ± 1.1[b]
Met	22.2 ± 2.9[b]	13.9 ± 1.6[b,d]	24.7 ± 1.9	31.5 ± 2.7[b,d]	4.7 ± 0.5	6.8 ± 0.7[b,d]
ML	21.8 ± 2.6[b]	17.8 ± 2.6[b,c]	25.1 ± 2.2	28.7 ± 2.4[b]	4.8 ± 0.5	7.7 ± 0.7[b]
MM	22.1 ± 2.5[b]	14.6 ± 1.8[b,d]	24.7 ± 2.1	30.2 ± 2.3[b,c]	4.7 ± 0.6	7.0 ± 0.6[b,c]
MH	21.7 ± 3.0[b]	13.5 ± 1.9[b,d]	24.8 ± 1.9	33.1 ± 2.9[d]	4.9 ± 0.6	6.5 ± 0.8[b,d]

Values are mean ± SEM (n = 10). NC, normal control group; DC, diabetic control group; Met, metformin-treated diabetic group; ML, diabetic group treated with 50 mg/kg MAP; MM, diabetic group treated with 100 mg/kg MAP; MH, diabetic group treated with 200 mg/kg MAP.
[a] $p < 0.05$ versus NC.
[b] $p < 0.01$ versus NC.
[c] $p < 0.05$ versus DC.
[d] $p < 0.01$ versus DC.

2.9. Cytokines assay

TNF-α, IL-6, and MCP-1 levels in the serum were determined by the sandwich ELISA method using commercially available kits. All appropriate standards and controls as specified by the manufacturer's kit were used. The data are expressed as picogram per milliliter serum.

2.10. Lipid peroxidation, SOD and glutathione peroxidase (GPx) activity detection

Lipid peroxidation was determined by measuring malondialdehyde (MDA) by its reaction with thiobarbituric acid. Thiobarbituric acid reactive substances (TBARS) were measured by a commercially available kit from Nanjing Jiancheng Bioengineering Institute according to the manufacturer's instructions, and expressed as the content of MDA in nanomoles per milliliter serum (Placer, Cushman, & Johnson, 1966). SOD and GPx activities were determined by using commercially available kits from Nanjing Jiancheng Bioengineering Institute according to the manufacturer's instructions.

2.11. Glycogen content analysis

Glycogen contents in the liver were measured using a glycogen assay kit (Biovision) according to the manufacturer's instructions.

2.12. Real-time reverse transcription-polymerase chain reaction (RT-PCR) analysis

Total RNA was isolated from the liver using TRIzol reagent and real-time quantitative RT-PCR was performed as described previously (Zhou, He, & Huang, 2009). The primers used for PCR were: GAPDH 5′-ttcaccaccatggagaaggc-3′ (forward) and 5′-ggcatggactgtggtcatga-3′ (reverse), phosphoenolpyruvate carboxyl kinase (PEPCK) 5′-tgcccaagatcttccatgtc-3′ (forward) and 5′-tccacctccttctcccaga-3′ (reverse) (Shin et al., 2011). All PCRs were performed in triplicate, and the thermal cycle conditions were as follows: 95 °C for 1 min followed by 40 cycles of 95 °C for 15 s and 60 °C for 1 min. Expression levels of PEPCK were corrected by normalization to the expression levels of the housekeeping gene GAPDH, and relative expression levels were calculated with the $2^{-\Delta\Delta Ct}$ rule (Livak & Schmittgen, 2001).

2.13. Immunohistochemistry

The thoracic aortas from the animals were dissected, fixed in 4% paraformaldehyde for 16 h, and embedded in paraffin. Sections (4 μm thick) were deparaffinized, rehydrated, and microwaved in citrate buffer for antigen retrieval. Sections were successively incubated in endogenous peroxidase block buffer, protein block buffer, and then with anti-CD68 antibody overnight at 4 °C. After rinsing in wash buffer, sections were incubated with labeled polymer-horseradish peroxidase anti-rabbit antibody and DAB chromogen. After the final wash, the sections were counterstained with hematoxylin. Finally, the slides were observed under a light microscope (Nikon Eclipse TE2000-U, NIKON, Japan). The images were examined (200× magnification) and evaluated for pathological changes.

2.14. Statistical analysis

Data are expressed as means ± SEM. Statistical analysis was performed by one-way analysis of variance (ANOVA) followed by Tukey post hoc test, if appropriate. A value of $p < 0.05$ was considered statistically significant.

3. Results and discussion

3.1. MAP decreased blood glucose levels, food intake, and increased body weights in diabetic mice

We first investigated the effect of MAP on FBG levels in STZ-induced diabetic mice. As shown in Table 1, compared with normal control mice, STZ-induced diabetic mice exhibited significantly increased FBG levels. However, MAP administration for 4 weeks led to a significant and dose-dependent fall in FBG levels in diabetic mice. Moreover, the hypoglycemic activity of MAP at a dose of 200 mg/kg seems to be comparable to that of metformin (150 mg/kg).

Next, we further measured body weights and food intake of mice. As shown in Table 1, compared with normal control mice, STZ-induced diabetic mice exhibited significantly decreased body weights and increased food intake, suggesting typical features of type 1 diabetes. Intriguingly, MAP administration (100 and 200 mg/kg) can significantly improve the weight loss in diabetic mice, which may be attributed to the ability of MAP to significantly improve glucose homeostasis. Furthermore, MAP administration (100 and 200 mg/kg) also reversed the elevated food intake in diabetic mice ($p < 0.05$ or $p < 0.01$), suggesting amelioration of diabetes.

3.2. Effect of MAP on blood TG, TC, LDL-C and HDL-C levels in diabetic mice

Elevated TC, LDL-C, TC/HDL-C ratio, and low HDL-C are well established risk factors for coronary heart disease (CHD) (Castelli et al., 1986; Kinosian, Glick, & Garland, 1994; Wilson et al., 1998). We next determined the serum lipid levels in control, diabetic, and MAP-treated mice. As shown in Table 2, compared with

Table 2
Effect of MAP administration for 4 weeks on serum lipid levels in STZ-induced diabetic mice.

Group	TG (mmol/L)	TC (mmol/L)	HDL-C (mmol/L)	LDL-C (mmol/L)
NC	0.93 ± 0.21	2.35 ± 0.44	1.25 ± 0.27	0.66 ± 0.18
DC	1.60 ± 0.28[b]	5.10 ± 0.89[b]	0.73 ± 0.20[b]	1.22 ± 0.17[b]
Met	1.05 ± 0.18[d]	3.04 ± 0.51[d]	1.19 ± 0.18[d]	0.75 ± 0.14[d]
ML	1.35 ± 0.23[a]	3.67 ± 0.48[b,c]	0.88 ± 0.12[a]	0.90 ± 0.16[c]
MM	1.18 ± 0.15[c]	3.31 ± 0.45[a,d]	1.02 ± 0.16	0.83 ± 0.15[d]
MH	1.09 ± 0.16[d]	2.87 ± 0.52[d]	1.16 ± 0.21[d]	0.71 ± 0.19[d]

Values are mean ± SEM (n = 10). NC, normal control group; DC, diabetic control group; Met, metformin-treated diabetic group; ML, diabetic group treated with 50 mg/kg MAP; MM, diabetic group treated with 100 mg/kg MAP; MH, diabetic group treated with 200 mg/kg MAP.
[a] $p < 0.05$ versus NC.
[b] $p < 0.01$ versus NC.
[c] $p < 0.05$ versus DC.
[d] $p < 0.01$ versus DC.

normal control mice, STZ-induced diabetic mice exhibited significantly increased TG, TC and LDL-C levels, as well as significantly decreased HDL-C levels. However, MAP administration significantly lowered TG, TC and LDL-C levels in diabetic mice in a dose-dependent manner, and significantly increased HDL-C levels in diabetic mice, suggesting improvement of dyslipidemia. After treatment with 200 mg/kg MAP for 4 weeks, the serum lipid levels in the diabetic mice restored to near normal levels, which were also comparable to those in metformin-treated diabetic mice.

3.3. MAP elevated serum and pancreatic insulin levels in diabetic mice

In type 1 diabetes, a high percentage of β cells are destroyed, and thus, there is little endogenous insulin production, leading to hyperglycemia and weight loss. To elucidate the mechanisms underlying the hypoglycemic effect of MAP in diabetic mice, we further determined the serum and pancreatic insulin levels in mice. As shown in Fig. 1, STZ-induced diabetic mice exhibited significantly lowered serum and pancreatic insulin levels compared with normal control mice. However, MAP administration (100 and 200 mg/kg) caused modest but significant elevation of serum insulin levels in diabetic mice (Fig. 1A). Likewise, the diabetic mice treated with MAP (100 and 200 mg/kg) also showed significant increases in pancreatic insulin contents compared with vehicle-treated diabetic mice (Fig. 1B), suggesting MAP can moderately enhance insulin synthesis and secretion in diabetic mice. This regulatory effect of MAP may contribute, at least in part, to its hypoglycemic effect in STZ-induced diabetic mice.

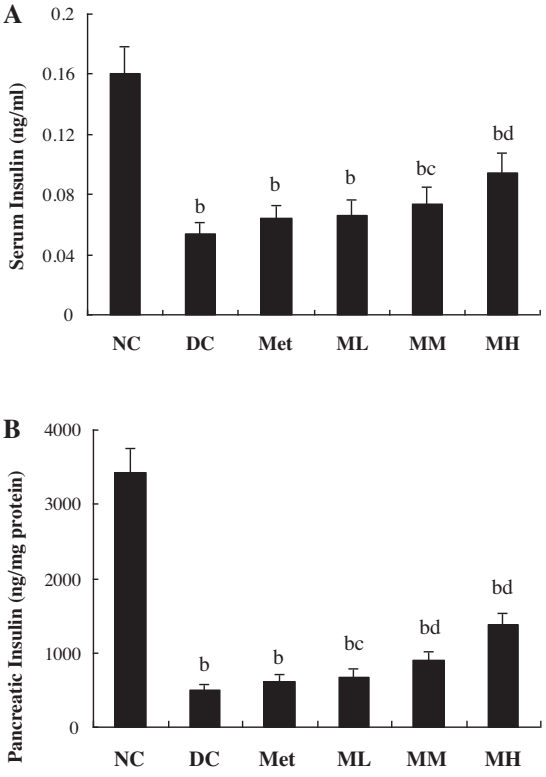

Fig. 1. Effect of MAP administration for 4 weeks on serum (A) and pancreatic insulin levels (B) in STZ-induced diabetic mice. NC, normal control group; DC, diabetic control group; Met, metformin-treated diabetic group; ML, diabetic group treated with 50 mg/kg MAP; MM, diabetic group treated with 100 mg/kg MAP; MH, diabetic group treated with 200 mg/kg MAP. Values are presented as mean ± SEM (n = 10). [b]$p < 0.01$, versus NC; [c]$p < 0.05$, [d]$p < 0.01$, versus DC.

3.4. Effect of MAP on MDA levels, SOD and GPx activities in serum and/or pancreata of diabetic mice

As shown in Table 3, STZ-induced diabetic mice exhibited significantly elevated serum MDA levels, and lowered SOD and GPx activities compared with normal control mice, similar to those observed in diabetic patients (Jain & McVie, 1999; Jay, Hitomi, & Griendling, 2006). However, the enhanced oxidative stress in diabetic mice was counteracted by MAP. MAP administration significantly decreased MDA levels, and elevated SOD and GPx activities in a dose-dependent manner in the blood of diabetic mice. Moreover, MAP administration also significantly lowered lipid peroxidation levels in the pancreata of diabetic mice.

Table 3
Effect of MAP administration for 4 weeks on serum MDA levels, SOD and GPx activities, and pancreatic MDA levels in STZ-induced diabetic mice.

Group	Serum			Pancreas
	MDA (nmol/mL)	SOD (U/mL)	GPx (U/mL)	MDA (nmol/mg protein)
NC	6.06 ± 0.69	180.6 ± 22.7	867.6 ± 93.3	0.94 ± 0.10
DC	11.67 ± 1.12[b]	85.3 ± 10.7[b]	521.9 ± 70.7[b]	4.14 ± 0.45[b]
Met	5.78 ± 0.71[d]	169.7 ± 18.9[d]	792.4 ± 95.3[d]	2.18 ± 0.38[b,d]
ML	8.13 ± 0.74[b,d]	120.4 ± 23.9[b,c]	677.4 ± 91.8[a]	3.25 ± 0.47[b,c]
MM	6.96 ± 0.82[d]	148.7 ± 16.4[d]	693.7 ± 96.1[c]	2.31 ± 0.31[b,d]
MH	5.58 ± 0.76[d]	167.2 ± 21.6[d]	765.4 ± 87.5[d]	1.97 ± 0.27[b,d]

Values are mean ± SEM (n = 10). NC, normal control group; DC, diabetic control group; Met, metformin-treated diabetic group; ML, diabetic group treated with 50 mg/kg MAP; MM, diabetic group treated with 100 mg/kg MAP; MH, diabetic group treated with 200 mg/kg MAP.
[a] $p < 0.05$ versus NC.
[b] $p < 0.01$ versus NC.
[c] $p < 0.05$ versus DC.
[d] $p < 0.01$ versus DC.

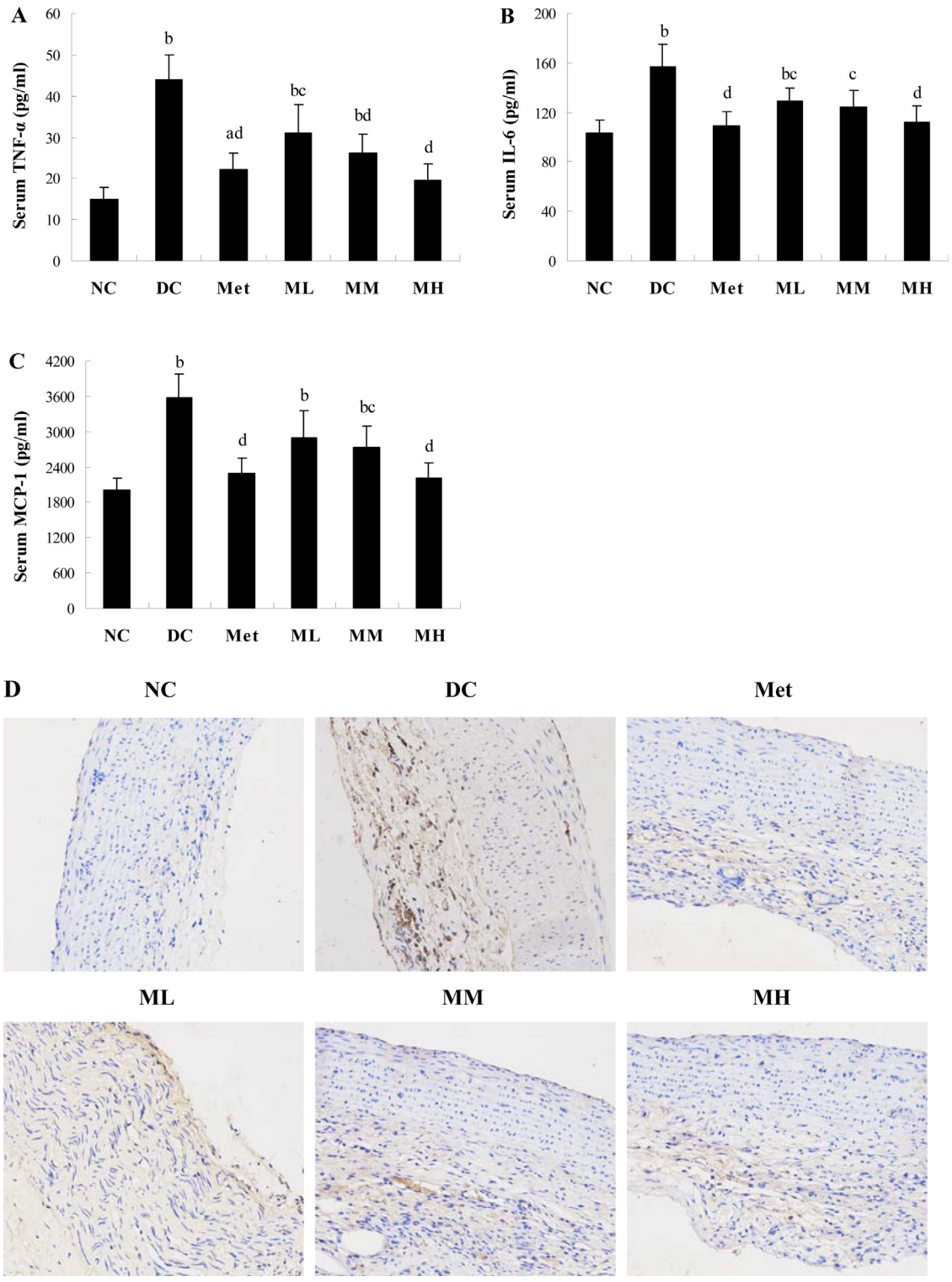

Fig. 2. Effect of MAP administration for 4 weeks on serum TNF-α (A), IL-6 (B) and MCP-1 (C) levels, and immunohistochemical staining for CD68 in the thoracic aortas (D) in STZ-induced diabetic mice. NC, normal control group; DC, diabetic control group; Met, metformin-treated diabetic group; ML, diabetic group treated with 50 mg/kg MAP; MM, diabetic group treated with 100 mg/kg MAP; MH, diabetic group treated with 200 mg/kg MAP. Values are presented as mean ± SEM ($n = 10$). $^{a}p < 0.05$, $^{b}p < 0.01$, versus NC; $^{c}p < 0.05$, $^{d}p < 0.01$, versus DC.

Given that pancreatic β cells are low in antioxidant defense and susceptible to oxidative stress (Zhou, Huang, & Lei, 2013), inhibition of pancreatic MDA levels by MAP can at least in part explain the observed elevation of pancreatic insulin contents in MAP-treated diabetic mice.

3.5. MAP decreased blood TNF-α, IL-6 and MCP-1 levels, and CD68-positive staining area in the thoracic aortas in diabetic mice

TNF-α, IL-6, and MCP-1 play an important role in diabetes and the vascular inflammation process through their multiple actions (Andreozzi et al., 2006; Kern, Ranganathan, Li, Wood, & Ranganathan, 2001; Rader, 2000; Wellen & Hotamisligil, 2005). As shown in Fig. 2, there was significant increases in TNF-α, IL-6, and MCP-1 levels in blood of diabetic control mice compared with those of normal control mice, similar to those observed in diabetic patients (Guha, Bai, Nadler, & Natarajan, 2000; Jain, Kannan, Lim, McVie, & Bocchini, 2002). However, this was prevented in diabetic mice treated with MAP (Fig. 2A–C). This suggests that MAP administration can effectively lower circulating levels of markers of vascular inflammation in STZ-induced diabetic mice. To further elucidate whether the hypoglycemic effect of MAP was associated with decreased vascular inflammation, we performed immunohistochemical staining using antibody against macrophages (CD68) in the thoracic aortas. As anticipated, CD68-positive staining area in the thoracic aortas was far more extensive in diabetic control mice than in normal control mice (Fig. 2D). However, MAP administration markedly reduced CD68-positive staining area in the thoracic aortas, similar to the effect of metformin treatment. Taken together, these data suggest that MAP administration could effectively improve vascular inflammation in STZ-induced diabetic mice.

In type 1 diabetes, elevated levels of both glycemia and ketosis can cause excessive oxygen radical production, and consequently increased oxidative stress (Brownlee, 2005; Guha et al., 2000; Jain, 1989; Jain, Kannan, & Lim, 1998; Jain & McVie, 1999; Jain, McVie, Jackson, Levine, & Lim, 1999; Jay et al., 2006; King & Loeken, 2004). Furthermore, oxidative stress can also increase the secretion of proinflammatory cytokines, and thus plays a key role in the regulatory pathways that progress from hyperglycemia to monocyte and endothelial cell activation in the enhanced vascular inflammation of diabetes (Brownlee, 2005; Jain, Rains, & Croad, 2007; Jain, Rains, Croad, Larson, & Jones, 2009). Our study demonstrates that MAP administration results in a significant inhibition of oxidative stress and proinflammatory cytokines in diabetic mice. The precise mechanism by which MAP inhibits proinflammatory cytokines is unknown and needs to be investigated. However, it is assumed that the inhibitory effect of MAP on proinflammatory cytokines may be mediated partly by inhibition of oxidative stress.

3.6. MAP inhibited PEPCK mRNA expression and increased glycogen contents in liver of diabetic mice

Blood glucose homeostasis is maintained by the balance between the rate of glucose entering the circulation (glucose appearance) and the rate of glucose clearance from the circulation (glucose disappearance). Gluconeogenesis is highly responsible for hepatic glucose production, an essential mechanism for the maintenance of blood glucose concentrations (Agius, 2007; Newsholme & Dimitriadis, 2001). PEPCK, a key gluconeogenic enzyme, has been found to be elevated in diabetic individuals. In line with this, excessive hepatic gluconeogenesis and glucose production are important contributors to diabetic hyperglycemia. Moreover, mammalian cells store glycogen in the liver for the production of glucose 6-phosphate during glycolysis (Okamoto et al., 2009).

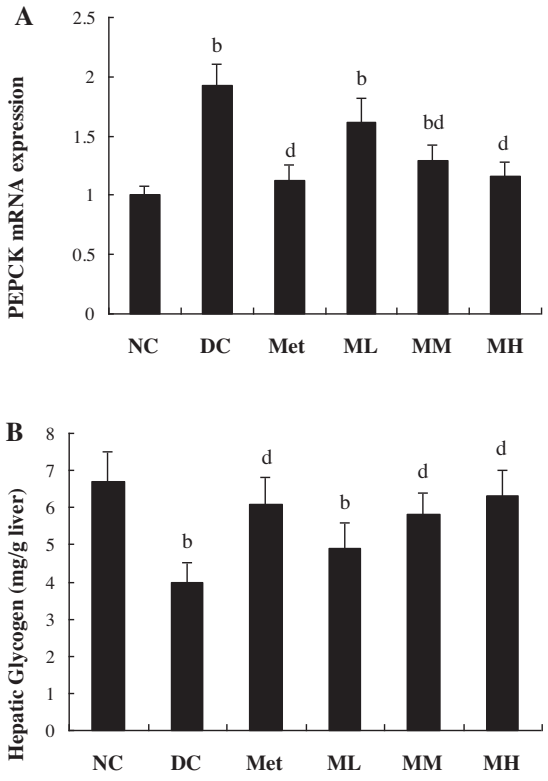

Fig. 3. Effect of MAP administration for 4 weeks on hepatic PEPCK mRNA expressions (A) and glycogen contents (B) in STZ-induced diabetic mice. NC, normal control group; DC, diabetic control group; Met, metformin-treated diabetic group; ML, diabetic group treated with 50 mg/kg MAP; MM, diabetic group treated with 100 mg/kg MAP; MH, diabetic group treated with 200 mg/kg MAP. Values are presented as mean ± SEM ($n = 10$). $^{b}p < 0.01$, versus NC; $^{d}p < 0.01$, versus DC.

In the current study, we further tested whether hepatic glycogen synthesis and gluconeogenesis-related signal molecule are involved in the hypoglycemic effect of MAP. As shown in Fig. 3, compared with normal control mice, the diabetic control mice exhibited significantly elevated PEPCK mRNA expression and lowered glycogen contents in the liver, consistent with the findings of other researchers (Hsu et al., 2013; Liu, Chang & Chiang, 2010). However, MAP administration (100 and 200 mg/kg) significantly reversed the increased PEPCK mRNA expression in the liver of diabetic mice (Fig. 3A). Furthermore, MAP administration (100 and 200 mg/kg) significantly enhanced the reduced glycogen contents in the liver of diabetic mice (Fig. 3B). These results indicate that MAP possesses the ability to reduce liver gluconeogenesis and promote hepatic glycogen synthesis, which may further contribute to the decrease in diabetic hyperglycemia.

3.7. MAP improved liver function and renal function markers in diabetic mice

Diabetes is known to be a metabolic disorder and is complicated by multi-organ deterioration. Accumulating evidence has suggested that oxidative stress and inflammation may play major roles in diabetes complications (Huerta & Nadler, 2004). In the current study, we tested the effects of MAP on liver function (AST, ALT) and renal function markers (BUN, creatinine) in diabetic mice. The data showed that MAP is capable of reversing the increased serum levels of ALT, AST, BUN and creatinine in diabetic mice (Table 4), indicating that MAP possesses potential hepatorenal protective action during diabetes. This is due, at least in part, to the inhibitory effects of MAP on vascular inflammation and oxidative stress in diabetic mice. However, whether MAP can ameliorate related diabetic

Table 4
Effect of MAP administration for 4 weeks on liver function and renal function markers in STZ-induced diabetic mice.

Group	AST (IU/L)	ALT (IU/L)	BUN (mg/dL)	creatinine (mg/dL)
NC	132.4 ± 17.8	65.4 ± 7.7	23.5 ± 1.9	0.25 ± 0.03
DC	261.2 ± 32.6[b]	227.8 ± 31.4[b]	45.6 ± 4.8[b]	0.38 ± 0.04[b]
Met	154.6 ± 24.2[d]	98.3 ± 15.3[b,d]	28.8 ± 3.0[b,d]	0.28 ± 0.03[d]
ML	212.4 ± 25.3[b]	171.0 ± 23.4[b,c]	37.5 ± 3.1[b,c]	0.32 ± 0.04[a]
MM	187.3 ± 26.8[b,d]	133.8 ± 15.6[b,d]	32.4 ± 3.6[b,d]	0.30 ± 0.04[c]
MH	165.9 ± 22.9[d]	116.8 ± 16.7[b,d]	29.6 ± 2.7[b,d]	0.26 ± 0.04[d]

Values are mean ± SEM (n = 10). AST, aspartate aminotransferase; ALT, alanine aminotransferase; BUN, blood urea nitrogen; NC, normal control group; DC, diabetic control group; Met, metformin-treated diabetic group; ML, diabetic group treated with 50 mg/kg MAP; MM, diabetic group treated with 100 mg/kg MAP; MH, diabetic group treated with 200 mg/kg MAP.

[a] $p < 0.05$ versus NC.
[b] $p < 0.01$ versus NC.
[c] $p < 0.05$ versus DC.
[d] $p < 0.01$ versus DC.

complications by protecting from oxidative stress and/or inflammation needs to be clarified in the future.

4. Conclusions

In the present study, we demonstrate for the first time the potential mechanisms responsible for the hypoglycemic activity of MAP in STZ-induced type 1 diabetic mice. Mechanistically, on the one hand MAP administration caused a significant elevation of serum insulin levels and pancreatic insulin contents in diabetic mice. On the other hand, MAP reversed the increased PEPCK mRNA expression and the reduced glycogen contents in the liver of diabetic mice. Thus, the antidiabetic activity of MAP is associated with elevated pancreatic insulin synthesis and secretion, elevated liver glycogen synthesis, and diminished liver gluconeogenesis. Moreover, MAP also improved the circulating levels of markers of vascular inflammation and oxidative stress in diabetic mice, which may contribute to the anti-diabetic effect of MAP. In addition, MAP also significantly improved the impaired liver function and renal function markers in the blood of diabetic mice. Taken together, these findings provide important new insights into the hypoglycemic activity and the underlying mechanisms of MAP in type 1 diabetic mice, and indicate that MAP may be a potential therapeutic option for type 1 diabetes. However, more studies are needed to further assess the mechanisms of action, structure-function relationship of MAP, and the efficacy of MAP administration as an adjuvant therapy for diabetic patients.

Conflicts of interest statement

The authors declare that there are no conflicts of interest.

Acknowledgments

The research was supported by grants from the National Natural Science Foundation of China (Nos. 21001045 and 31270870). We thank the staff from Analytical and Testing Center of Huazhong University of Science and Technology for their assistances in real-time PCR experiments.

References

Agius, L. (2007). New hepatic targets for glycaemic control in diabetes. *Best Practice & Research Clinical Endocrinology & Metabolism*, *21*, 587–605.

Andreozzi, F., Laratta, E., Cardellini, M., Marini, M. A., Lauro, R., Hribal, M. L., et al. (2006). Plasma interleukin-6 levels are independently associated with insulin secretion in a cohort of Italian-Caucasian nondiabetic subjects. *Diabetes*, *55*, 2021–2024.

Brownlee, M. (2005). The pathogenesis of diabetic complications: A unifying mechanism. *Diabetes*, *54*, 1615–1625.

Castelli, W. P., Garrison, R. J., Wilson, P. W., Abbott, R. D., Kalousdian, S., & Kannel, W. B. (1986). Incidence of coronary heart disease and lipoprotein cholesterol levels. The Framingham Study. *JAMA*, *256*, 2835–2838.

Chen, X., Tang, J., Xie, W., Wang, J., Jin, J., Ren, J., et al. (2013). Protective effect of the polysaccharide from *Ophiopogon japonicus* on streptozotocin-induced diabetic rats. *Carbohydrate Polymers*, *94*, 378–385.

Fu, J., Yuan, J., Tu, Y. Y., Fu, J., Zhang, N., Gao, B., et al. (2012). A polysaccharide from *Acanthopanax senticosus* improves the antioxidant status in alloxan-induced diabetic mice. *Carbohydrate Polymers*, *88*, 517–521.

Goto-Nance, R., & Watanabe, Y. (1995). Characterization of lectins from the skin mucus of the loach, *Misgurnus anguillicaudatus*. *Fish Sciences*, *61*, 137–140.

Guha, M., Bai, W., Nadler, J. L., & Natarajan, R. (2000). Molecular mechanisms of tumor necrosis factor alpha gene expression in monocytic cells via hyperglycemia-induced oxidant stress-dependent and -independent pathways. *Journal of Biological Chemistry*, *275*, 17728–17739.

Hsu, F. L., Huang, C. F., Chen, Y. W., Yen, Y. P., Wu, C. T., Uang, B. J., et al. (2013). Antidiabetic effects of pterosin A, a small-molecular-weight natural product, on diabetic mouse models. *Diabetes*, *62*, 628–638.

Huerta, M. G., & Nadler, J. L. (2004). Oxidative stress, inflammation and diabetic complications. In D. LeRoith, S. I. Taylor, & J. M. Olefsky (Eds.), *Diabetes Mellitus: A Fundamental and Clinical Text* (pp. 1485–1501). Philadelphia: Lippincott Williams & Wilkins.

Hurtley, S., Service, R., & Szuromi, P. (2001). Cinderella's coach is ready. *Science*, *291*, 2337–2343.

Jain, S. K. (1989). Hyperglycemia can cause membrane lipid peroxidation and osmotic fragility in human red blood cells. *Journal of Biological Chemistry*, *264*, 21340–21345.

Jain, S. K., Kannan, K., & Lim, G. (1998). Ketosis (acetoacetate) can generate oxygen radicals and cause increased lipid peroxidation and growth inhibition in human endothelial cells. *Free Radical Biology and Medicine*, *25*, 1083–1088.

Jain, S. K., Kannan, K., Lim, G., McVie, R., & Bocchini, J. A. (2002). Hyperketonemia increases TNF-α secretion in cultured U937 monocytes and type-1 diabetic patients. *Diabetes*, *51*, 2287–2293.

Jain, S. K., & McVie, R. (1999). Hyperketonemia can increase lipid peroxidation and lower glutathione levels in human erythrocytes in vitro and in type 1 diabetic patients. *Diabetes*, *48*, 1850–1855.

Jain, S. K., McVie, R., Jackson, R., Levine, S. N., & Lim, G. (1999). Effect of hyperketonemia on lipid peroxidation levels of plasma in diabetic patients. *Diabetes Care*, *22*, 1171–1175.

Jain, S. K., Rains, J. L., & Croad, J. L. (2007). Effect of chromium nicinate and chromium picolinate supplementation on lipid peroxidation, TNF-α, IL-6 CRP, glycated hemoglobin, and cholesterol levels in blood of streptozotocin-treated diabetic rats. *Free Radical Biology and Medicine*, *43*, 1124–1131.

Jain, S. K., Rains, J., Croad, J., Larson, B., & Jones, K. (2009). Curcumin supplementation lowers TNF-α, IL-6, IL-8, and MCP-1 secretion in high glucose-treated cultured monocytes and blood levels of TNF-α IL-6, MCP-1, glucose, and glycosylated hemoglobin in diabetic rats. *Antioxidants & Redox Signaling*, *11*, 241–249.

Jay, D., Hitomi, H., & Griendling, K. K. (2006). Oxidative stress and diabetic cardiovascular complications. *Free Radical Biology and Medicine*, *40*, 183–192.

Kern, P. A., Ranganathan, S., Li, C., Wood, L., & Ranganathan, G. (2001). Adipose tissue tumor necrosis factor and interleukin-6 expression in human obesity and insulin resistance. *American Journal of Physiology: Endocrinology and Metabolism*, *280*, E745–E751.

Kimura, M., Hama, Y., Sumi, T., Asakawa, M., Rao, B. N., Horne, A. P., et al. (1994). Characterization of a deaminated neuraminic acid-containing glycoprotein from the skin mucus of the loach, *Misgurnus anguillicaudatus*. *Journal of Biological Chemistry*, *269*, 32138–32143.

King, G. L., & Loeken, M. R. (2004). Hyperglycemia-induced oxidative stress in diabetic complications. *Histochemistry and Cell Biology*, *122*, 333–338.

Kinosian, B., Glick, H., & Garland, G. (1994). Cholesterol and coronary heart disease: Predicting risks by levels and ratios. *Annals of Internal Medicine*, *121*, 641–647.

Liu, S. H., Chang, Y. H., & Chiang, M. T. (2010). Chitosan reduces gluconeogenesis and increases glucose uptake in skeletal muscle in streptozotocin-induced diabetic rats. *Journal of Agricultural and Food Chemistry*, *58*, 5795–5800.

Livak, K. J., & Schmittgen, T. D. (2001). Analysis of relative gene expression data using real-time quantitative PCR and the $2^{-\Delta\Delta Ct}$ method. *Methods*, *25*, 402–408.

Newsholme, E. A., & Dimitriadis, G. (2001). Integration of biochemical and physiologic effects of insulin on glucose metabolism. *Experimental and Clinical Endocrinology & Diabetes*, *109*, S122–S134.

Noh, J. R., Hwang, J. H., Kim, Y. H., Kim, K. S., Gang, G. T., Kim, S. W., et al. (2013). The orphan nuclear receptor small heterodimer partner negatively regulates pancreatic beta cell survival and hyperglycemia in multiple low-dose streptozotocin-induced type 1 diabetic mice. *International Journal of Biochemistry & Cell Biology*, *45*, 1538–1545.

Okamoto, T., Kanemoto, N., Ban, T., Sudo, T., Nagano, K., & Niki, I. (2009). Establishment and characterization of a novel method for evaluating gluconeogenesis using hepatic cell lines, H4IIE and HepG2. *Archives of Biochemistry and Biophysics*, *491*, 46–52.

Okutumi, T., Nakajima, Y., Sakakibara, F., Kawauchi, H., & Yamazaki, M. (1987). Induction of a cytotoxin from murine bone narrow by an animal lectin. *Cancer Research*, *47*, 47–50.

Park, C. B., Lee, J. H., Park, I. Y., Kim, M. S., & Kim, S. C. (1997). A novel antimicrobial peptide from the loach *Misgurnus angullicaudatus*. *FEBS Letters*, *411*, 173–178.

Placer, Z. A., Cushman, L. L., & Johnson, B. C. (1966). Estimation of product of lipid peroxidation (malonyl dialdehyde) in biochemical systems. *Analytical Biochemistry*, *16*, 359–364.

Qin, C., Ding, Y., Huang, K., & Xu, H. (2008). Protective effect of *Misgurnus anguillicaudatus* polysaccharide on immunological liver injury in mice. *International Immunopharmacology*, *8*, 607–612.

Qin, C. G., Huang, K. X., & Xu, H. B. (2002a). Effects of *Misgurnus anguillicaudatus* polysaccharides on glycemia and lipidemia in experimental diabetic mice. *Chinese Journal of Pharmacology and Toxicology*, *16*, 124–127.

Qin, C. G., Huang, K. X., & Xu, H. B. (2002b). Investigation on immunomodulating activities of polysaccharide from loach mucus. *Chinese Pharmaceutical Journal*, *37*, 588–591.

Qin, C., Huang, K., & Xu, H. (2002c). Isolation and characterization of a novel polysaccharide from the mucus of the loach, *Misgurnus anguillicaudatus*. *Carbohydrate Polymers*, *49*, 367–371.

Qin, C., Huang, K., & Xu, H. (2002d). Protective effect of polysaccharide from the loach on the in vitro and in vivo peroxidative damage of hepatocyte. *Journal of Nutritional Biochemistry*, *13*, 592–597.

Qin, C. G., Zhou, J., Zhao, W., Huang, K. X., & Xu, H. B. (2001). Effects of the loach polysaccharide on removal of reactive oxygen species and protection of DNA chains. *Acta Biochimica et Biophysica Sinica*, *33*, 215–218.

Rader, D. J. (2000). Inflammatory markers of coronary risk. *New England Journal of Medicine*, *343*, 1179–1182.

Shin, H., Park, Y. H., Kim, S. U., Moon, H. B., Park, do S., Han, Y. H., et al. (2011). Hepatitis B virus X protein regulates hepatic glucose homeostasis via activation of inducible nitric oxide synthase. *Journal of Biological Chemistry*, *286*, 29872–29881.

Wellen, K. E., & Hotamisligil, G. S. (2005). Inflammation, stress, and oxidative stress. *Journal of Clinical Investigations*, *115*, 1111–1119.

Whitear, M. (1984). Biology of the integument 2. In J. Bereiter-Hahn, A. G. Matoltsy, & K. S. Richards (Eds.), *Vertebrates* (pp. 8–38). Berlin: Springer-Verlag.

Wilson, P. W. F., D'Agostino, R. B., Levy, D., Belanger, A. M., Silbershatz, H., & Kannel, W. B. (1998). Prediction of coronary heart disease using risk factor categories. *Circulation*, *97*, 1837–1847.

Zhang, C. X., & Huang, K. X. (2005). Apoptosis induction of a novel polysaccharide from the mucus of the loach, *Misgurnus anguillicaudatus* on HL-60 cells. *Journal of Ethnopharmacology*, *99*, 385–390.

Zhang, C., & Huang, K. (2005). Characteristic immunostimulation by MAP, a polysaccharide isolated from the mucus of the loach, *Misgurnus anguillicaudatus*. *Carbohydrate Polymers*, *59*, 75–82.

Zhang, C. X., & Huang, K. X. (2006). Mechanism of apoptosis induced by a polysaccharide, from the loach *Misgurnus anguillicaudatus* (MAP) in human hepatocellular carcinoma cells. *Toxicology and Applied Pharmacology*, *210*, 236–245.

Zhang, W., Zheng, L., Zhang, Z., & Hai, C. X. (2012). Protective effect of a water-soluble polysaccharide from *Salvia miltiorrhiza* Bunge on insulin resistance in rats. *Carbohydrate Polymers*, *89*, 890–898.

Zhou, J., He, X., & Huang, K. (2009). Bidirectional regulation of insulin receptor autophosphorylation and kinase activity by peroxynitrite. *Archives of Biochemistry and Biophysics*, *488*, 1–8.

Zhou, J., Huang, K., & Lei, X. G. (2013). Selenium and diabetes – Evidence from animal studies. *Free Radical Biology and Medicine*, *65*, 1548–1556.

Zhu, J., Liu, W., Yu, J., Zou, S., Wang, J., Yao, W., et al. (2013). Characterization and hypoglycemic effect of a polysaccharide extracted from the fruit of *Lycium barbarum* L. *Carbohydrate Polymers*, *98*, 8–16.